CHAPTER 5

DESIGN APPROACH AND BEAM-WAVE INTERACTION STUDIES OF THE TUNABLE-FREQUENCY GYROTRONS FOR DNP-NMR SPECTROSCOPY APPLICATIONS

5.1. Introduction

As discussed in Chapter 1 of this thesis, gyrotron oscillators are the potential RF sources for various applications that require RF power at either single frequency or tunable frequency range. The inclusion of Dynamic Nuclear Polarization (DNP) mechanism makes the use of Nuclear Magnetic Resonance (NMR) spectroscopy very wide by enhancing the sensitivity of the signal. But the DNP driven NMR spectroscopy requires either a tunable NMR magnet or a tunable RF source. Comparatively, the design, development and maintenance of a tunable RF source have large and many benefits, like, simple and reliable over tunable NMR magnet systems. Gyrotron oscillators are capable of generating a low power over a band frequency tuning range and enhance the sensitivity and the realization of DNP-NMR spectroscopy more effectively.

Dynamic Nuclear polarization is a key technique which transfers unpaired electrons spin polarization into nuclear spins and is used for the enhancements of sensitivity of NMR spectroscopy study that enables faster data acquisitions in various sample characterization. For the enhanced sensitivity study of DNP-NMR spectroscopy, a RF source is required at the NMR frequencies. In addition to this, a DNP NMR spectroscopy requires either a super conducting NMR magnet with sweep coils or a tunable RF source for the study of various samples. Due to the complexities involved in the arrangements of a tunable NMR magnet, now the researches are also focussed on the development of various tunable RF microwave sources at various NMR frequencies.

Gyrotron is the most suitable RF source for this application. The gyrotron research is now getting focussed to play its role in DNP-NMR spectroscopy where a few watts to several tens of watts of CW RF power required over a tunable bandwidth. Several gyrotron oscillators for the DNP-NMR applications have been analyzed,

designed and experimentally investigated at electron frequencies 132 GHz, 260 GHz, 330 GHz, 460 GHz, etc[Hornstein,(2001)].

In this Chapter, the design of a tapered cavity RF interaction structure of gyrotron for 263 GHz for a 400 MHz NMR spectroscopy system is investigated. The operating mode is considered as $TE_{5,3,q}$ with a target of more than 2 GHz tunable bandwidth. The tunability of the device is studied by magnetic tuning as well as electrical tuning methods.

The presented chapter is organized as follows. Section 5.2 contains the various tunable techniques used in gyro-devices for achieving a tunability. In Section 5.3, the design of tapered cavity interaction structure along with its cold cavity analysis is presented. The beam wave interaction analysis using time dependent multimode theory given by Fliflet *et al.* (1991) for the proposed design is presented in Section 5.4 at various magnetic and beam voltage variations.

5.2. Tuning Techniques Used for the DNP Gyrotrons

The main aim of any tunable RF source is to provide desired amount of RF power over a wide range of frequencies. Generally, shift in the frequencies and power levels are achieved by varying the beam parameters. In the case of gyrotron oscillators, since the device is based on the CRM instability principle, where the exchange of power between RF wave and electron beam depends on the frequency of oscillation of the mode as well as the cyclotron frequency of oscillation. The operating frequency of gyrotron mainly depends on the resonating frequency of the RF interaction cavity and the cyclotron frequency of the electrons that are interacting with the RF fields generated by the noise inside the interaction structure. Hence, by allowing the variations in either resonating frequency of the interaction cavity mode or cyclotron frequency of the electrons, the tunability of the device can be achieved.

There are several techniques used in general for achieving the tunability of the device in gyrotrons, namely, mechanical and thermal tuning methods which affect the dimensions of the interaction cavity thereby resonating frequency of the mode, and by electrical and magnetic tuning methods which yields the variations in the cyclotron frequency of the electrons thereby shift in the operating frequency of the device. A brief description of these tuning techniques used in the gyrotrons is presented as follows [Dumbrajs *et al.* (2011)].

5.2.1. Mechanical Tuning

As the name indicates, in the mechanical tuning, the frequency tuning is achieved by inducing changes in the cavity dimension mechanically and simultaneously adjusting the strength of the magnetic field B(z) as well as the beam parameters. The DC magnetic field along the cavity is adjusted here in order to maintain the synchronism between the interaction mode and the electrons. Since, the variations in the cavity dimension directly effects the oscillating frequency of the mode thereby shifts in the operating frequency.

For a rigid cavity type, it is unattainable to change the transverse dimensions because of lack of provisions for altering the cavity dimensions and results in implementation of mechanical tuning impossible. However, an effective transverse dimension alteration can be made with a split cavity structure. Here, frequency tuning is achieved by sliding the wedge shaped pieces pneumatically, so that the two halves are moved apart or closer by the necessary amount to affect the transverse dimensions thereby the frequency of operation. But the presence of gap in the cavity restricts the operation of the device to azimuthally non-symmetric modes [Dumbrajs *et al.* (2011)]. Apart from limited modes of operation, the major challenge with the mechanical tuning is the handling of cooling system which is responsible for longer life of the RF cavity.

In high power gyrotrons, the resonators must be rigorously cooled so as to limit any uncontrollable changes of their dimensions due to overheating. It is difficult to maintain the mechanical changes of the cavity along with the cooling system. Due to this, the mechanical tuning method is limited to low power, and short pulse gyrotrons only where the role of cooling is minimal. In spite of this, implementation of mechanical tuning is easy in the quasi optical gyrotron where the distance between the mirrors to be modified which makes the Fabry-Perot resonator. So this type of tuning is most suitable for quasioptical gyrotrons and unfeasible for a tapered cavity and coaxial cavity gyrotrons.

5.2.2. Thermal Tuning

In thermal tuning method, the variations in the operating frequencies are achieved by allowing the variations in temperatures of the coolant along the interaction structure and thereby controlling the impact of the ohmic losses in the interaction cavity due to RF power generation that leads to mechanical deformations of the cavity, as discussed, in Chapter 3 and Chapter 4.

Alteration in temperature of the coolant, results in variation in the temperature of the interaction structure wall due to variable amount of heat exchange in the system. According to the property of thermal coefficient of expansion of the cavity material, there is contraction or expansion of the walls as per the temperature variations. These changes in the cavity dimensions result variation in the resonating frequency of the mode of the structure which in turn results in variation in the operating frequency of the device. The amount of tuning achieved via thermal technique mainly depends on the cavity material properties. Considering the tolerances in the cavity dimensions, the amount of frequency shift is very small.

It has been reported that a 4 MHz /^{o} C of frequency shift is obtained in the low power gyrotrons operating at 263 GHz [Glyavin *et al.* (2015)]. In the case of moderate lengths interaction structure, this technique is found suitable for tuning since, operation on high order axial modes are limited. For 140 GHz gyrotron reported by Joye *et al.* (2006) mentioned that they achieved frequency tuning via thermal variations. The thermal and mechanical tuning techniques directly affects the resonating frequencies of the mode and do not affect the cyclotron frequencies of the electrons.

5.2.3. Electrical Tuning

In electrical tuning, the DC voltage of the electron beams varied thus the cyclotron frequency of the electrons are get altered that results shift in the frequency of energy exchange, i. e., the operating frequency of the device. It is one of the most widely used techniques for achieving the frequency tenability in the gyrotrons. The variations in the beam accelerating potential leads to the changes in the relativistic factor, γ, and is given by as follows [Edgcombe (1993)]:

$$\gamma = 1 + \frac{V_b}{m_e c^2}, \tag{5.1}$$

where V_b is the beam voltage, m_e is the rest mass of electron and c is velocity of light in free space. The variations in the relativistic mass factor γ effects the cyclotron frequency of the electrons and is known by

$$\Omega = \frac{eB_0}{m_e \gamma_0} \approx 28s \frac{B_0[\mathrm{T}]}{\gamma}[\mathrm{GHz}], \tag{5.2}$$

where s is the harmonic number, B_0 is the external DC magnetic field. From the above equations (5.1) and (5.2), it is obvious that the variation in the accelerating voltage result the variations in relativistic factor there by the variations in the cyclotron frequency. As the energy exchange depends on the synchronous condition between

cyclotron frequency of the electron beam and the resonating frequency of the mode, these variations affects the operating frequency.

Percentage variation in the relativistic factor with the variations in DC beam voltage is determined by

$$\frac{d\gamma}{\gamma_0}\times 100 \approx \frac{dV_b}{511+V_{b0}}\times 100 \ . \tag{5.3}$$

Here, γ_0 and V_{b0} are the initial relativistic mass factor and beam voltages. The percentage of variation in cyclotron frequency for the variations in beam voltage is given by

$$\frac{d\Omega}{\Omega_0}\times 100 \approx -\frac{dV_b}{511+V_{b0}}\times 100 \ . \tag{5.4}$$

Here, Ω_0 is the initial cyclotron frequency of electrons and negative sign in equation (5.4) indicates the increase in beam voltages yields reduction in cyclotron frequency. Equations (5.3) and (5.4) specifies that the amount of variations in the cyclotron frequency is not only depends on the amount of variation in the beam voltages but also on the starting values of beam voltage.

Figure 5.1 shows the effect of the beam voltage variations on the relativistic factor and cyclotron frequency of the device with the start value of beam voltage is 15 kV (random value). It is observed that typically for this case, 1 kV change of beam voltage nearly yields a 0.175% change in both cyclotron frequency as well as relativistic factor keeping the rest of beam parameters as constant. Since the intensity of electric fields can be changed very rapidly which results smaller switching times means that faster electrical tuning. But it requires a very sensitive and expensive power supplies which makes the realization of frequency tunability through the electrical tuning complex.

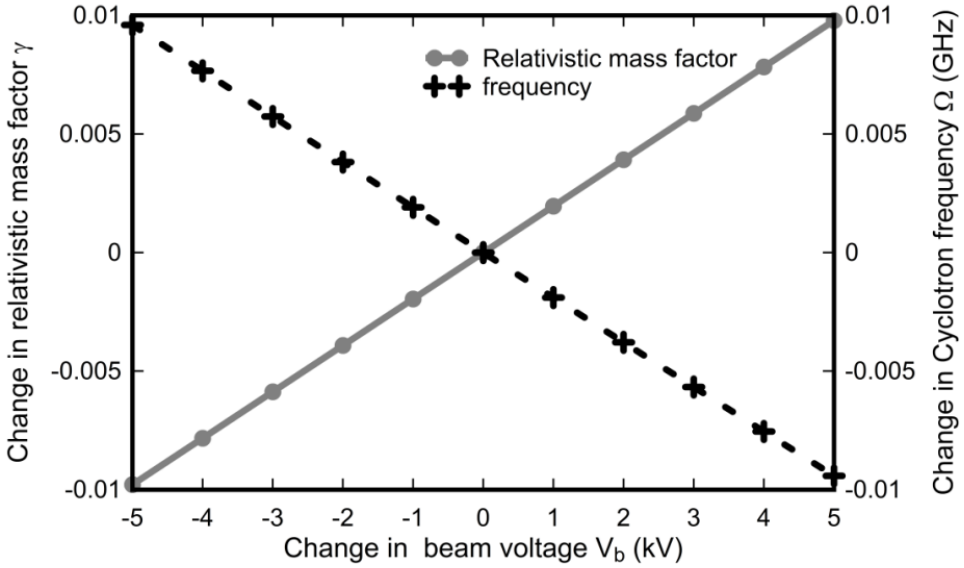

Figure 5.1: Dependence of relativistic factor and cyclotron frequency with respect to beam voltage.

5.2.4. Magnetic tuning

Similar to electrical tuning, the magnetic tuning also yields variation in cyclotron frequency of electrons thereby variations in the operating frequency of the device by altering the magnetic field B along the interaction structure.

Equation (1.2), indicates that the variations in cyclotron frequency are directly proportional to the variations in magnetic field. Thus, magnetic tuning is simple and more effective to achieve higher tunable frequency because of the ease of varying magnetic field though having the longer switching times between different magnetic field values. The percentage of variation in cyclotron frequency for the variations in beam voltage is given by

$$\frac{d\Omega}{\Omega_0}\times 100 = \frac{dB}{B_0}\times 100 \quad . \tag{5.5}$$

Here, B_0 means the starting value of B from which the variations starts. The equation (5.5), indicates that the amount of variations in the cyclotron frequency is not only

depends on the amount of variation in the magnetic field but also on the starting values of beam voltage.

The percentage variation in the cyclotron frequency with the magnetic field is shown in figure 5.2. It can be observed that 1% of change in cyclotron frequency is produced with the change of magnetic field of 0.01 Tesla with the reference value of B_0 = 1 T, which has a strong effect on frequency compared to the beam voltage.

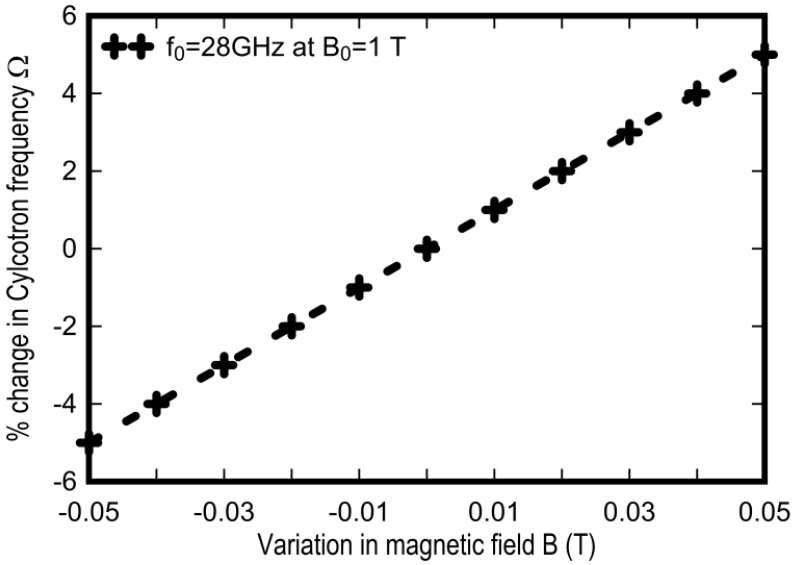

Figure 5.2: Percentage change of cyclotron frequency versus magnetic field B (T).

In this Chapter, a tapered cylindrical RF cavity is designed for achieving a continuous tunable bandwidth using both the magnetic and electrical tuning for a 400MHz NMR spectroscopy applications.

5.3. Design Constraints and Mode Selection for the Tunable Frequency Gyrotrons

Like in the high power gyrotrons discussed in Chapter 3 and Chapter 4, for the low power tunable gyrotron purposes also, a cylindrical tapered RF section has been considered as the interaction structure of the gyrotron. In the continuous tunable gyrotrons, tunability has been achieved by incorporating different tunable techniques as

discussed above, through exciting device in the high order axial mode indices with fixed azimuthal and radial variations. For the generation of high order axial modes, long interaction cavity sections needed usually, of the order of few tens of operating wave length. As well, the diffraction losses that results the RF power reduces as the axial mode index increases and which needs a proper selection of beam parameters along with suitable cavity geometry.

In the Chapter, the design and analysis of the RF interaction cavity structure for the 400MHz DNP enhanced NMR spectroscopy applications presented. The $TE_{5,3,q}$ mode, at the 263 GHz operating frequency along with beam parameters have been taken from the experimental data [Glayvin *et al.* (2015)], here *q* indicates the number of axial variations in the field across interaction cavity. The design investigation is carried out with the aim of a tunable bandwidth greater than 2 GHz via magnetic, electrical tuning.

In this Chapter, as mentioned above, the operating mode is chosen as $TE_{5,3,q}$ [Glayvin *et al.* (2015)]. With the help of coupling coefficient curves, the optimum beam radius that allows maximum coupling between beam and RF wave has been chosen and are plotted in figure 5.3 for various normalized beam radius $\overline{R_b} = R_b / R_c$.

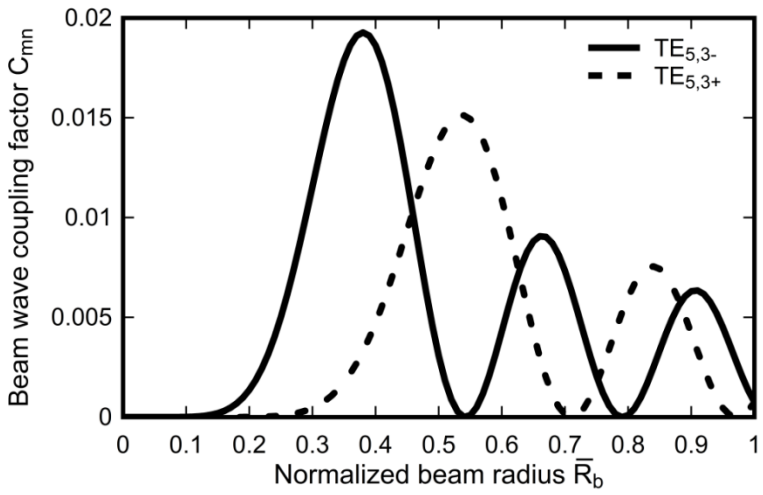

Figure 5.3: Beam wave coupling factor C_{mn} versus normalized beam radius $\overline{R_b} = R_b / R_c$

Observing beam wave coupling dependence of the mode, the beam radius is taken as 0.96 mm which is at the first radial maximum and will be optimized by the inspection of beam wave interaction studies in the following sections.

5.3.1. Design of Tunable RF Cavity Structure

The design parameters are taken from the Glyavin *et al.* (2015) and are tabulated in Table 5.1. The optimization of axial RF cavity dimensions are calculated by solving the single mode Vlasov approximation equation for various cavity dimensions as discussed in Chapter 3. Dimensions of the tapered cylindrical RF cavity are optimized for $TE_{5,3,q}$ choosing cavity interaction length 22.49 mm (~20 λ), and the optimized dimensions are tabulated in Table 5.2.

Table 5.1: Design constraints

Parameter	Value
Frequency	263
Tunable bandwidth	>2GHz
Pitch factor	1.5
Beam voltage	10-15kV
Beam current	20-50 mA
Magnetic field	9.6-9.7
Beam radius	0.96 mm

Table 5.2: RF Interaction parameters

Parameter	Value
Down taper angle θ_d (^{0})	2
Uptaper angle θ_{up} (^{0})	0.8
Down taper length, L_d (mm)	15
Uptaper length, L_{up} (mm)	25
Middle section length L_c (mm)	22.49
Cavity radius (mm)	2.54

Table 5.3: Q_{diff} and f_{res} for various axial mode indices q of TE_{53q}

Axial Mode index, q	Frequency, GHz	Q_{diff} factor
1	262.9780	14500
2	263.182	3510
3	263.527	1660
4	264.005	950
5	264.621	605
6	265.377	436

The normalized axial field profiles for various high order q along the interaction structure are plotted in Figure 5.4. The corresponding Q_{diff} and resonating frequencies f_{res} are determined and tabulated in Table 5.3. It is observed that as the q increases, the value $Q_{diff,q}$ reduces as well the oscillating frequency of the mode increasing.

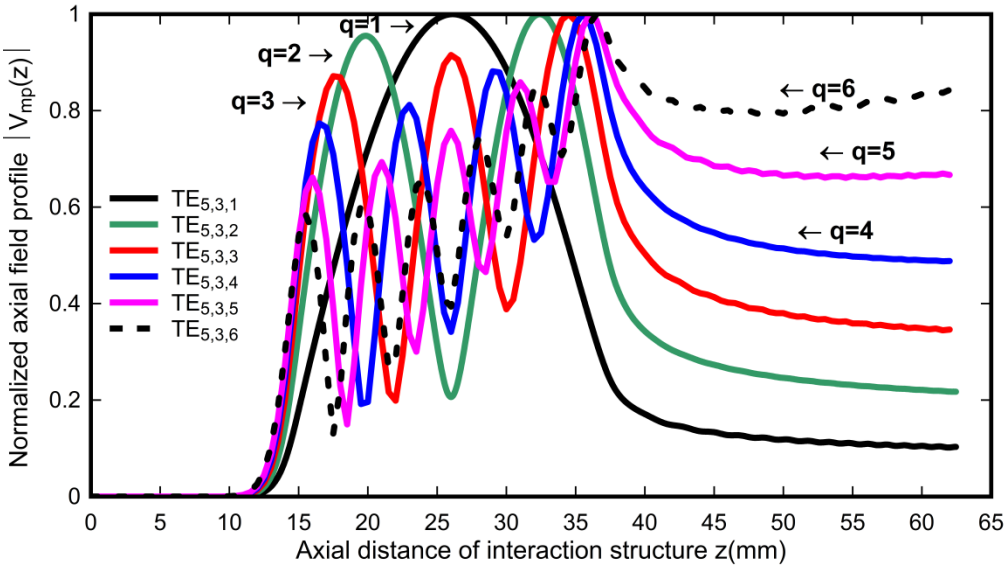

Figure 5.4: Axial mode profiles at beam absent conditions for various q of proposed RF interaction cavity.

5.3.2. Start Oscillation Currents for the Higher-Order Axial Mode Indices

Now, like in the previous chapters, the start oscillation curves used for determining compete modes as well the minimum currents needed for the growth of several modes at various magnetic fields are determined. Unlike, single axial mode index i.e., q = 1, the I_{soc} curves are determined using (3.9) and (3.10) equations, but for the present work, the device should operate in various axial mode indices for tunability. Hence, the field profile used for deriving equations (3.9) and (3.10) are need to modify that results calculation of I_{soc} for q >1 values. According to Torrezan *et al.* (2010), the I_{soc} for various high order axial mode indices q are determined by using the following expressions.

$$I_{soc} = -\frac{1}{2}\left(\frac{m_e \varepsilon_0 c^3}{e}\right)\left(\frac{\gamma_0}{Q}\right)\left(\frac{s!2^s}{s^s}\right)^2 \frac{\beta_{\perp 0}^{2(3-s)}}{C_{m,p}} \frac{\left(\frac{\pi^2}{\lambda}\right)\int_0^L |h(z)|^2 dz}{\left(s+\frac{\partial}{\partial \Delta}\right)\left|\int_0^{\mu} h(\zeta)\exp\left(j\int_0^{\zeta}\Delta d\zeta'\right)d\zeta\right|^2} \qquad (5.6)$$

where, s gives harmonic number, C_{mp} is the coupling coefficient, and the rest of the parameters are already defined in Chapter 3 of this thesis; h (z) indicates the axial field profile in the interaction cavity. By providing the h (z) profiles evaluated from Vlasov approximation equations, the I_{soc} curves are determined for the various axial mode indices. The diffractive quality factor Q values are also updated as for the q. The start oscillation current I_{soc} are calculated for the beam parameters mentioned in Table 5.4 by varying magnetic fields 9.5 to 9.9 T and are plotted in Figure 5.5. It has been detected that the operated mode is significantly differ from various compete mode and shows a promise for more tunability with respect to magnetic tuning. As well, it is observed that a minimum beam current of 20 mA, will excites the axial modes q = 1 to 6. All the modes are distinguished curves with respect to magnetic field that gives the confirmation about the oscillation of various modes along the interaction structure.

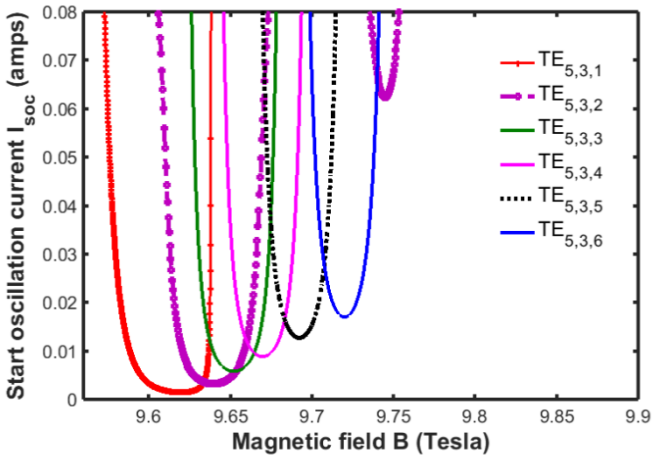

Figure 5.5: Start Oscillation currents for $TE_{5,3,q}$ mode q = 1 to 6 versus magnetic field.

Later, the voltage depression V_{dep} for various beam currents is determined and the % percentage of V_{dep} with respect to the beam voltages V_b is plotted in Figure 5.6. It is observed that as the beam current increases the amount of voltage depression also increase though all are in very much lower to the maximum allowed limit.

From the design and analysis of RF cavity, it has been observed that the proposed RF cavity can be operated over a various axial modes and allows a tuning bandwidth of 2.4 GHz. Though, the proposed RF cavity supports growth of various axial mode indices, but it is the responsibility of the beam parameters (especially V_b) and magnetic fields (B(z)) to make it possible. In the present work, by incorporating the electrical tuning, magnetic tuning as well the hybrid tuning, the proposed cavity has been investigated for various input parameters (combinations of beam voltage, magnetic field as well both) . Since, considering the limitations of time and complexities with computational resources available, for the present work, the beam wave interaction studies are carried out with help of the time dependent multimode theory and are discussed in detail in the following section.

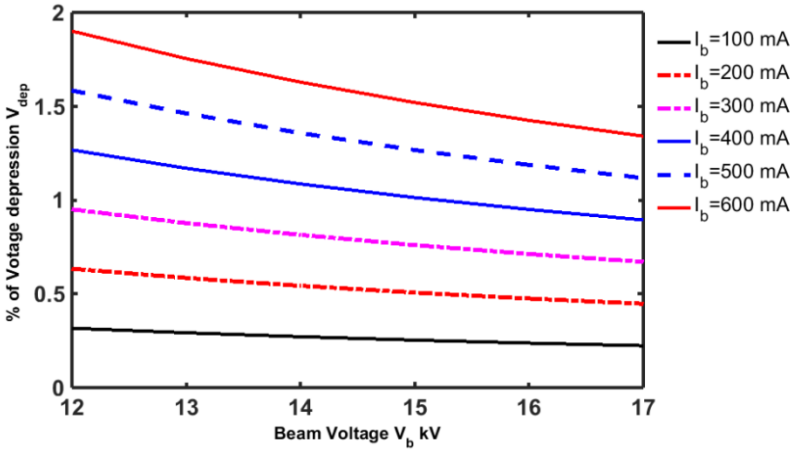

Figure 5.6: % of voltage depression versus beam voltages for the various beam current values.

5.4. Analytical Studies of the Beam-Wave Interaction

The cold cavity analysis in the former section confirms that the interaction structure is suitable for generating the high order axial mode profiles of q = 1 to 6. The mode profile of various axial variations with the resonating frequencies mentioned in table that allows a possible tunable bandwidth of > 2.3 GHz. In the present work, the beam wave interaction studies for the proposed cavity have been performed using the nonlinear time dependent multimode theory discussed in Chapter 3. For the beam interaction studies, considering the field profile h (z) at various q, the multimode analysis theory has been carried out performed for various beam parameters. With beam current of 400 mA, the initial beam wave interaction studies are done and later on the beam current have been reduced in the steps and finally the beam currents are settled to 20 mA.

5.4.1. Investigations via Magnetic Tuning

Like presented in chapter 3 and Chapter 4, the beam wave interaction studies are carried out by considering 32 beamlets and 32 electrons for each beam let. The investigation are started by providing beam currents, I_b = 0.4 A, the tunability of proposed RF interaction of gyrotron are investigated by magnetic as well as electrical tuning for 400 MHz DNP-NMR spectroscopies.

Considering the magnetic tuning first, the magnetic fields along the interaction structure is varied in order to tune the mode of operation at different frequencies. The output power developed in the interaction mode, $TE_{5,3,q}$ for q =1 to 6 for the interaction structure tabulated in Table 5.2 are performed. In Figure 5.7, in addition to RF output power level, the oscillation frequencies of various axial modes are also shown with respect to the magnetic field. Initially, considering I_b = 400 mA, the beam wave interactions are carried out. Later, the beam currents are reduce in steps and the RF

power levels and corresponding frequencies at beam current 20 mA are calculated and are plotted in Figure 5.8.

Table 5.4: Magnetic tuning parameters at I_b = 400 mA

Axial Variation, q	Frequency (GHz)	Magnetic Field (T)	Beam Voltage (kV)	RF Output Power (kW)	$Q_{diff,q}$ Quality factor
1	262.9780	9.6050	15	1.0516	14500
2	263.1817	9.6120	15	1.001	3510
3	263.523	9.6255	15	0.9891	1560
4	264	9.64159	15	0.9871	890
5	264.620	9.6675	15	0.881	562
6	265.370	9.7005	15	0.490	412

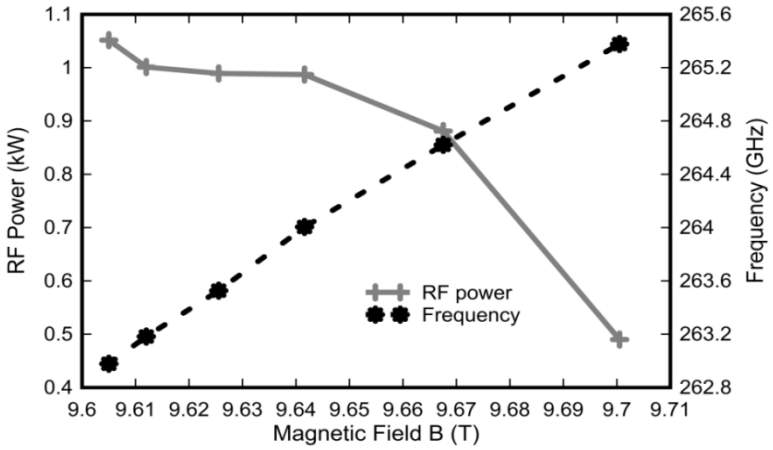

Figure 5.7: Operating frequencies and RF power levels for various axial variations, q =1 to 6 in magnetic tuning at I_b = 400mA.

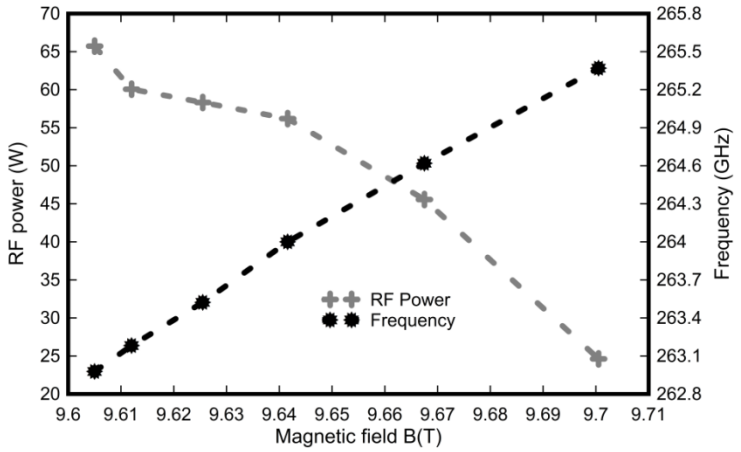

Figure 5.8: Operating frequencies and RF power levels for various axial variations, q = 1 to 6 in magnetic tuning at I_b = 20 mA.

5.4.2. Investigations via Electrical Tuning

Secondly, the tunability of the proposed design is studied for beam voltage variations namely electrical tuning. As per the beam voltage variations, the RF power developed in interaction cavity mode $TE_{5,3,q}$, from q = 1 to 6, is tabulated in Table 5.5, which gives the various RF power levels for different axial variation modes at various oscillating frequencies.

Table 5.5: Electrical tuning parameters

Axial Mode q	Frequency (GHz)	Magnetic Field (T)	Beam Voltage (kV)	RF Output Power (kW)	Q_{diff} Quality factor
1	262.9780	9.605	15	1.0516	14500
2	263.1817	9.605	14.590285	0.9862	3510
3	263.523	9.605	13.904195	0.9732	1560
4	264	9.605	12.9538	0.9079	890
5	264.620	9.605	11.734129	0.8085	562
6	265.370	9.605	10.244976	0.7039	412

It can be observed from Figures 5.9 and 5.10 that variations in the RF power output as well as oscillating frequencies with respect to the variations in the beam voltage at I_b = 400 mA as well I_b = 25 mA.

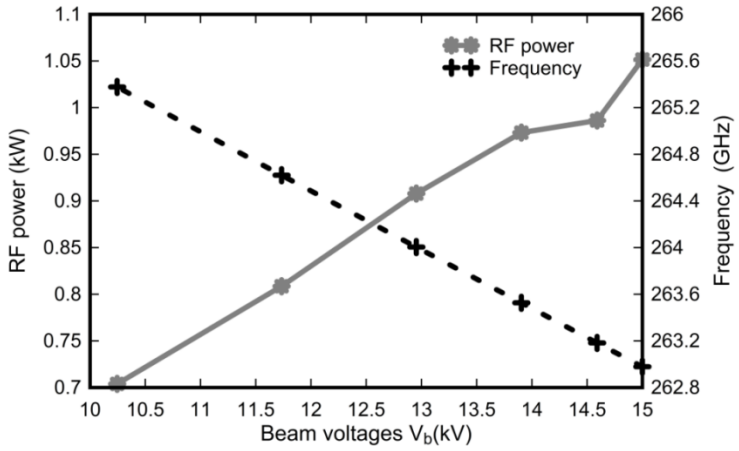

Figure 5.9: Resonant frequencies and RF power levels for various axial variations, q =1 to 6 in electrical tuning at I_b= 400 mA.

It can be further observed that, the magnetic tuning results good amount of power over electrical tuning even though both tuning mechanisms resulting a significant amount power more than 490 W at I_b = 400 mA as well around 50W threshold power at I_b = 0.02A.

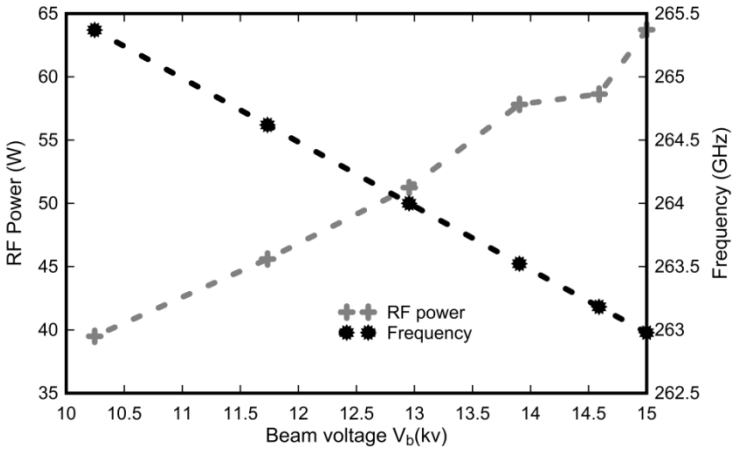

Figure 5.10: Resonant frequencies and RF power levels for various axial variations, q = 1 to 6 in electrical tuning at Ib = 20 mA.

5.5. Output RF Window

For the present work too, a single disc type RF window has been chosen for transmitting the generated RF power in the device to the output transmission line. Considering the broadband tunability nature of RF output, the design has been carried for several disc thicknesses d_w. As well, since the generated RF power does not cause any thermal deformations so no cooling has been necessary. For the present case, a SiO_2 Corning 7980 UV has been chose as a window material. The material properties have been tabulated in Table 5.6 [Mandal *et al.* (2015) and Gray *et al.* (2008)].

Table 5.6: SiO_2 Window for $TE_{5,3,q}$ mode

Material	**Window radius R_{win}**	**Permittivity**	**Loss tangent**	**d_0, disk thick ness at N=1**
SiO_2	25.75 mm	3.9	115×10^{-5}	0.2888 mm

By means of the analysis presented in Chapter 2, the transmission T(dB) and reflection characteristics R (dB) of output RF window versus frequencies at various disc thicknesses d_w has been investigated .

The disc thickness is given by

$$d_w = N\frac{c}{2f\sqrt{\varepsilon_r}}, \quad \text{where } d_0 = \frac{f}{2f\sqrt{\varepsilon_r}} \quad , \tag{5.7}$$

where N is an integer and varies, 1, 2, 3, 4, ... etc.

In the present work, N has been has been varied from 1 to 8 for identification of suitable disc thickness. The window has been designed by assuming the generated RF power is in TEM_{00} mode at the RF window. The radius of the window is chosen as 25.75 mm, even though the radius of the RF window does not effect in case of TEM_{00} mode.

The resulted reflection and transmission characteristics versus frequency for various thicknesses are plotted in Figures 5.11 and 5.12.

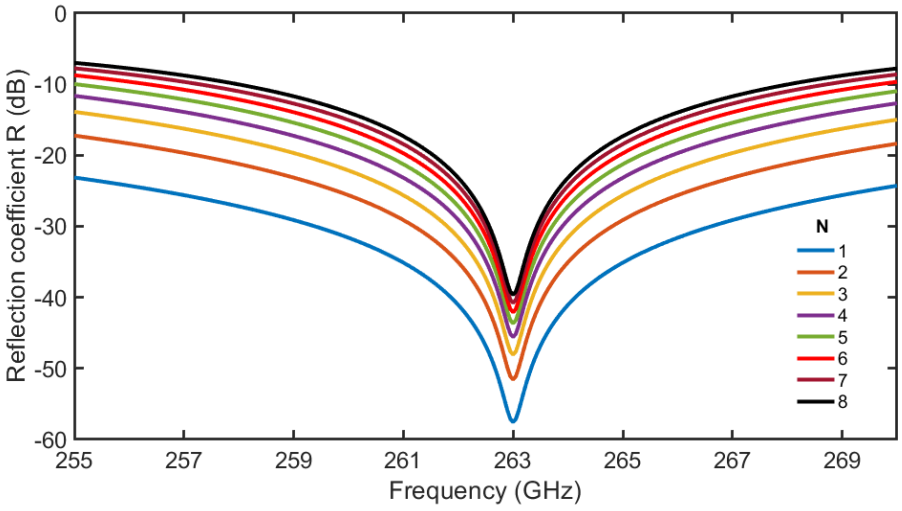

Figure 5.11: Reflection characteristics R (dB) versus frequency (GHz) at various disc thickness $d_w = N^* d_0$ of window radius thickness.

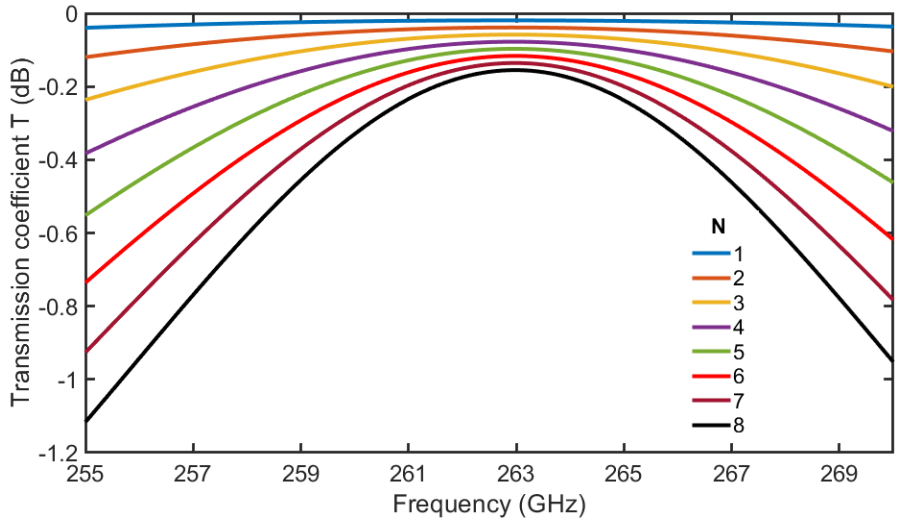

Figure 5.12: Transmission characteristics T (dB) versus frequency (GHz) at various disc thickness $d_w = N*d_0$.

It can be observed that the variation in the disc thickness are effecting the transmission characteristics of maximum variation of 0.25dB per d_0 variation multiple whereas the reflection characteristics all are having minimum value at 263 GHz and the amount of reflection increases with the disc thickness. By observing, the window thickness has been chosen for $N = 4$, i. e., $d_w = 1.155$ mm for the window radius of 25.75 mm.

5.6. Conclusions

The design constraints, design and analysis of RF interaction cavity structure of the tunable gyrotrons for the DNP-NMR spectroscopy applications are presented. Initially, for the operated mode $TE_{5,3,q}$, the RF interaction structure has been determined by solving single mode Vlasov approximation for various cavity geometries and are optimized. Later, for identifying the minimum beam currents and various competing modes, the linear theory of gyrotrons has been used and the corresponding parameters

for various axial mode indices of the operating mode are determined. As of now, the time dependent multimode theory has been used for deciding the working modes with single axial mode index, i. e., $q = 1$. By amending necessary changes to the time dependent multimode theory, i. e., updating Gaussian profiles to the actual *h(z)* profiles for various axial mode, variations of the beam wave interactions are carried out. The magnetic and electrical tuning techniques have been implemented for achieving the broadband tunability. In case of magnetic tuning, by varying a *B(z)* from 9.6005 T to 9.7005 T, a continuous frequency band of 2.4 GHz has been observed. For the case of electrical tuning technique, by down shifting the beam voltage from 15 kV to 10.245 kV, a continuous tunability of 2.4 GHz has been achieved with threshold of output power >20 W. All the analysis has been carried out considering zero spread in the beam as well no misalignments in between the beam optical axis and microwave circuit axis. Since, the generated output power is very less that it does not cause severe deformations in the structure by ohmic losses so the thermal analysis has not been performed.

As well as, the output RF window that acts as shielding between the vacuumed and outside transmission system has been designed using SiO_2, Corning 7980 UV as material. For various cavity thicknesses, the reflection and transmission characteristics of the window versus frequency have been performed and the optimized window parameters are determined.